

# Synthesis, characterization, and its PL dynamics of colloidal type II CdTe/CdSe nanocrystals

著者	Oda Masaru, Nishiyama Akira, Marumo Gi-ichi, Yamada Shuhei, Tanaka Erina, Tani Toshiro
journal or publication title	Physica Status Solidi C
volume	6
number	1
page range	61-64
year	2009-01
URL	<a href="http://hdl.handle.net/10228/00006906">http://hdl.handle.net/10228/00006906</a>

doi: info:doi/10.1002/pssc.200879878

# Synthesis, characterization, and its PL dynamics of colloidal type II CdTe /CdSe nanocrystals

Masaru Oda<sup>\*1,2</sup>, Akira Nishiyama<sup>2</sup>, Gi-ichi Marumo<sup>2</sup>, Shuhei Yamada<sup>2</sup>, Erina Tanaka<sup>2</sup>, and Toshiro Tani<sup>1,2</sup>

<sup>1</sup> Institute of Symbiotic Science and Technology, Division of Advanced Applied Physics, Tokyo University of Agriculture and Technology (TAT), Naka-cho 2-24-16, Kogane-i, Tokyo 184-8588, Japan

<sup>2</sup> Department of Applied Physics, TAT, Naka-cho 2-24-16, Kogane-i, Tokyo 184-8588, Japan

Received 9 July 2008, revised 1 August 2008, accepted *zzz*

Published online *zzz*

PACS 78.67.Bf, 78.67.Hc, 78.55.Et, 68.47.Fg

\* Corresponding author: e-mail odamasa@cc.tuat.ac.jp, Phone: +81 42 388 7423, Fax: +81 42 385 6255

We describe our improved synthesis and optical properties of high quality type II CdTe/CdSe nanocrystals (NCs). Specifically, clear shell-thickness dependences have been observed in the absorption and photoluminescence (PL) spectra and PL decay profiles as well. The magnitude of the lowest absorption band decreases drastically with large redshift as the shell thickness increases. The origin will be discussed on the bases of the model where the spatial configuration of the lowest electron-hole pair in the NCs changes from that of type I to type II as the shell thickness increases. As for the PL lifetime of the lowest electron-hole excitations, substantial increase is observed with increasing shell thickness. This can also be understood by considering the spatial configuration; spatial overlap between electron and hole wavefunctions decreases with increasing shell thickness, thus the lifetime increases. As for the NCs with extremely thin shell ( $\square$  IML; IML = 0.35 nm), the PL lifetime seems much longer than expected. This suggests that the thin shells seem imperfect and work rather a kind of trap sites than layers.

Copyright will be provided by the publisher

**1 Introduction** Colloidal type II nanocrystals (NCs) have been expected to have fascinating optical properties which arise from spatial separations of strongly confined electrons and holes. Recently, in type II core-shell NCs, such as CdTe/CdSe and CdSe/ZnTe NCs, unique optical properties were observed, e.g. shifting of photoluminescence (PL) toward near infrared [1] and an optical gain in single-exciton regime [2].

It is important to fabricate and investigate the samples with high-quality heterointerface and well defined shell structure for further understandings of optical properties of the type II NCs, because the properties in type II NCs are more sensitive to the condition of the heterointerface and also of the shell than those in type I NCs.

We have improved the method of synthesis for high-quality type I CdSe/ZnS NCs [3] based on previous reports [4-7]. Here we describe at first our recent synthetic pathways for high-quality type II CdTe/CdSe NCs based on our method improved for the type I NCs. Optical properties such as absorption and PL spectra are presented, which are measured on so-obtained high-quality CdTe/CdSe NCs

with different shell thicknesses (1, 2, 3, 4, 6 and 8 ML, IML = 0.35 nm). We characterize the origin of observed two absorption bands and also a PL band from a comparison between experimental and theoretical results.

We describe shell thickness dependence of the PL decay profiles. Decay times increase basically as the shell thickness increases, while the NCs with IML shell seems exception. Possible mechanism of the PL dynamics in the CdTe/CdSe NCs will be discussed.

**2.1 Samples** There are two major improvements in our synthesis; one is that the purchased organic reagents are distilled prior to use for purification, and the other the different solvents are used in the core and shell growth processes, respectively, to get better achievement. The former contributes to increase the reproducibility of size and PL quantum yield, while the latter to decrease linewidths of absorption and PL spectra of the NCs.

**Chemicals and their preparations** The organic reagents, i.e. tri-n-octylphosphine oxide (TOPO) and hexadecylamine (HDA) are used as received from Dojin Chem-

Copyright line will be provided by the publisher

icals and Wako Chemicals, respectively. The reagents are purified by vacuum boiling and distillation.

Pre-diluted dimethylcadmium/triethylphosphine ( $\text{Me}_2\text{Cd}/\text{TOP}$ ) solution (1:25 vol. ratio) is purchased from Trichemical Research. Using the pre-diluted solution instead of non-diluted one reduces the risk due to pyrophoric nature of  $\text{Me}_2\text{Cd}$ . The solution is further diluted with TOP by a factor of 10 prior to use.

99.999 % Se (Wako Chemicals) and 99.9999 % Te (Furuuchi Chemicals) shots are used as received, respectively. Tri-n-octylphosphine (TOP) is purchased from Tokyo Kasei Kogyo. To prepare 1.0 M Te/TOP (Se/TOP) solution, mixture of 1.276 g Te (0.79 g Se) and 10 mL TOP are heated to 180 °C for 3 hours under Ar atmosphere. The solution is further diluted with TOP by a factor of 10 prior to use.

**Synthesis** Preparation of CdTe core-NCs proceeds as follows. 0.64 mL (0.34 mmol Cd)  $\text{Me}_2\text{Cd}/\text{TOP}$  solution and 0.24 mL (0.24 mmol Te) Te/TOP are mixed with 1.8 mL TOP and charged into a syringe in a drybox. The syringe is removed outside with rubber cap. The mixed solution is injected into a vigorously stirred mixture of 8g TOPO and 4g HDA heated at 120 °C under  $\text{N}_2$  gas in a flask. The injection resulted in an immediate nucleation of NCs. After the injection, the temperature is allowed to fall to 70 °C to prevent from further nucleation, and then is kept at 100 °C for 1 hour to grow NCs.

The CdSe shells are formed around the CdTe cores as follows. First, 2 mL of the above mentioned solution containing CdTe NCs is transferred to another flask which is pre-heated at 170 °C filled with 6 g pure TOPO under  $\text{N}_2$  gas. Separately, 0.072 mL (0.09, 0.103, 0.111, 0.244 and 0.263 mL)  $\text{Me}_2\text{Cd}/\text{TOP}$  solutions and 0.027 mL (0.034, 0.039, 0.042, 0.092 and 0.099 mL, respectively) TOP-Se solutions are mixed with 1 mL TOP and the mixture is charged into a syringe. Each solution is then added dropwise into the flask with an interval of 30 seconds. After the reaction, 2 mL solution containing CdTe/CdSe core-shell NCs is sampled. By repetition of the dropwise addition and sampling processes, six samples with different shell thickness were obtained subsequently.

After the growth processes, 1 mL anhydrous butanol was added to avoid solidification of TOPO at room temperature (RT). The NCs are purified by precipitation with 5 mL anhydrous methanol to rinse residual TOPO and HDA, and finally they are dispersed in 3 mL anhydrous toluene for optical measurements. All the optical measurements here were performed at RT.

**2.2 Quantum confinement in core-shell NCs** In order to characterize optical properties of CdTe/CdSe NCs, we simulated the lowest energy and wavefunction of an electron-hole pair in the core-shell NCs by a simple model calculation assuming spherical shapes of the NCs.

For simplify, we neglect Coulomb interaction effects between the electron-hole pairs. This assumption is applicable in the regime where the radius of NCs is smaller than

exciton Bohr radius ( $r_{\text{CdTe}}^{\text{Bohr}} = 6.8 \text{ nm}$ ), because the confinement effect is much larger than the effect of Coulomb interactions. Schrödinger equation for the electron and hole is expressed as

$$\left[ -\frac{\hbar^2}{2m_{e/h}^*} \nabla^2 + V_{e/h}(r) \right] \psi_{e/h}(r, \theta, \varphi) = E_{e/h} \psi_{e/h}(r, \theta, \varphi), \quad (1)$$

where  $\hbar$  and  $m_{e/h}^*$  are Dirac's constant and effective mass. Subscript  $e$  or  $h$  corresponds electrons or holes, respectively.  $V_{e/h}(r)$  is spherical square-well potential;

$$V_{e/h}(r) = V_{e/h}^{\text{core}}(r \leq a), V_{e/h}^{\text{shell}}(a < r \leq b), V_{e/h}^{\text{TOPO}}(r > b), \quad (2)$$

where  $a$  and  $b$  are radii of core and shell, respectively. In the present case,  $\psi_{e/h}(r, \theta, \varphi)$  is separated as

$$\psi_{e/h}(r, \theta, \varphi) = R_{e/h}(r) Y_{e/h}(\theta, \varphi), \quad (3)$$

where  $R_{e/h}(r)$  and  $Y_{e/h}(\theta, \varphi)$  are the radial wave function and spherical harmonic function, respectively. The  $R_{e/h}(r)$  should satisfy the boundary conditions [8]

$$\begin{cases} R_{e/h}^{\text{core}}(a) = R_{e/h}^{\text{shell}}(a) \\ \frac{1}{m_{e/h}^{*(\text{core})}} \frac{dR_{e/h}^{\text{core}}(r)}{dr} \Big|_{r=a} = \frac{1}{m_{e/h}^{*(\text{shell})}} \frac{dR_{e/h}^{\text{shell}}(a)}{dr} \Big|_{r=a} \end{cases}, \quad (4)$$

Using the wavefunctions derived from Eq. (4), the lowest state energy and  $|\psi_{e/h}(r, \theta, \varphi)|^2$  for electron and hole were evaluated. Parameters required for evaluations are described in the caption.

Figure 1(a) shows an estimated phase diagram for carri-

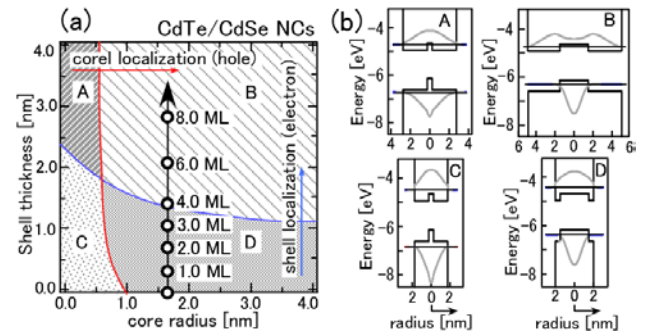


**Figure 1** (a) Localization phase diagram of carriers in CdTe/CdSe core-shell NCs. Circles indicate the data of the NCs used in this paper. The radius of the core CdSe is 1.65 nm. The thicknesses of the CdTe/CdSe NCs are 1, 2, 3, 4, 6, 8 ML, respectively.  $m_e^{*(\text{CdTe})}$ ,  $m_h^{*(\text{CdTe})} = 0.0963, 0.62$ .  $m_e^{*(\text{CdSe})}$ ,  $m_h^{*(\text{CdSe})} = 0.112, 0.45$ . (b) The values of conduction band minimum (CBM) and valence band maximum (VBM) energies of CdTe are  $-4.65 \text{ eV}$  and  $-6.15 \text{ eV}$ , respectively. Those of CdSe are  $-4.94 \text{ eV}$  and  $-6.62 \text{ eV}$ , and of organic molecules are  $-1 \text{ eV}$  and  $-16 \text{ eV}$ . The energy zero corresponds to the vacuum level. Grey lines show existence probability of an electron and a hole.

er configurations in CdTe/CdSe NCs. There are four regimes (A-D in Fig. 1(a)) in the diagram [2]. Grey lines in Fig. 1(b) show  $|\psi_{e \text{ or } h}(r, \theta, \varphi)|^2$  of carriers in the four regimes, respectively. In regime C, both electrons and holes are delocalized over the entire hetero-NC volume (type I-like excitons), while in B electrons and holes are localized in shell and core, respectively (type II-like excitons). Circles in Fig. 1(a) indicate the prepared points of the CdTe/CdSe NCs used in this work. As can be seen, the NCs with thicker CdSe shells ( $\geq 4ML$ ,  $1ML = 0.35 \text{ nm}$ ) are expected to be type II NCs.

**3 Results and Discussion** We describe first optical properties of well-defined type I CdSe/ZnS core-shell NCs. Figure 2(a) shows typical examples of absorption and PL spectra of our CdSe/ZnS NCs. The numbers in the figures indicate shell thicknesses of the NCs. Lowest absorption band (A) and higher band (B) are associated with the electron-hole pair excitations of a 1s-electron and a 1s-hole and of a 1p-electron and a 1p-hole, respectively [9].

The PL spectra in Fig. 2(a) show narrow and single lines. Their line-widths are almost similar to the corresponding absorption band A. The PL band is associated with a recombination of a spin-singlet 1s-electron and 1s-hole pairs, and Stokes shift between the absorption and the PL maxima is mainly due to electron-phonon coupling [10].

Both the lowest absorption band A and the PL band show little redshift less than 90 meV even changing the shell thickness. The small shell thickness dependence surely indicates that the electron and hole are both confined mostly within the core regions. Circles and squares in Fig. 2(c) show the peak energies of the absorption band A and the PL band, respectively. Solid line in Fig. 2(c) show the simulated energy dependence by the model described in §2.2. The calculation fits the experimental features quantitatively well.

Now we discuss the features observed in CdTe/CdSe NCs. Figure 2(b) show the absorption and PL spectra of the NCs in the present work. Although peak positions of the absorption maxima might not be legible due to the scale limitation, in the absorption spectra bands A (and B) are also feasible as indicated positions. Numerical calculations for non-coated CdTe NCs [9] suggest the existence of the bands A, B and others. So we conclude, for the moment, the observed bands A and B are the same origin as that of the CdSe/ZnS NCs.

The PL spectra show sharp and single lines with moderate dependence on the shell thickness. The sharpness indicates that the NCs possess good heterointerface and high-quality shell as well. Single lineshape ensures that no incidental nucleations of CdSe NCs take place during the growth of the CdSe shell. The PL band shift to the lower energy side appears systematically with increasing the shell thickness. It is clear the PL is neither due to defects nor impurities.

The overall redshift of the PL band is clearly seen in the order of 500 meV. The strong dependence on shell thickness can be interpreted qualitatively by considering that the

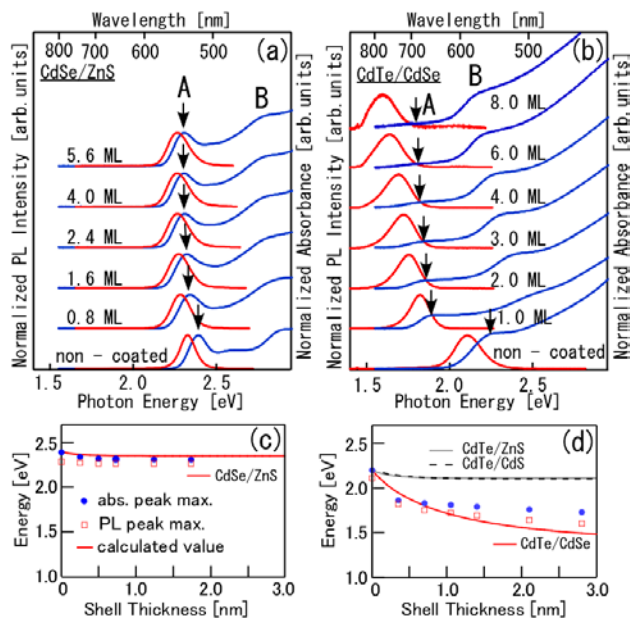


**Figure 2** Absorption and PL spectra of (a) CdSe/ZnS core-shell NCs ( $1 \text{ ML} = 0.31 \text{ nm}$ ) and (b) CdTe/CdSe core-shell NCs. Wavelength of the excitation light is 430 nm. ( $1 \text{ ML} = 0.35 \text{ nm}$ ). Arrows indicate absorption band maxima. (c), (d) Circles show the energies of the absorption maxima. Solid lines show the calculated value of the energies of confined electron-hole pair as a function of shell thickness. The radii of the core of CdSe and CdTe NCs are estimated as 2.7 nm and 1.65 nm from the comparison with the energies of absorption maxima of non-coated NCs with calculated values by Eqs. (1) and (4). The thicknesses of the shell were estimated from the mole-ratios between core and shell materials.  $m_e^{*(\text{ZnS})}$ ,  $m_h^{*(\text{ZnS})} = 0.28, 0.49$ .  $m_e^{*(\text{CdS})}$ ,  $m_h^{*(\text{CdS})} = 0.171, 0.7$ . The values of CBM and VBM energies of ZnS are  $-3.90 \text{ eV}$  and  $-7.52 \text{ eV}$ , respectively. Those of CdSe are  $-4.67 \text{ eV}$  and  $-7.13 \text{ eV}$ .

electron confinement in the shell region as expected (cf. regime B in Fig. 1(b)) and thus the energy is sensitive to the shell thickness. In addition, calculated curve based on the model in §2.2 fits fairly well the experimental trends as shown in Fig 2(d). It is noted that such large redshift can not be deduced if the NCs are type I NCs (see the calculations for type I CdTe/ZnS and CdTe/CdS NCs in Fig 2(d)).

In the absorption spectra, there is one more specific feature which supports that the CdTe NCs with a thick CdSe shell are type II NCs. Magnitude of the band A relative to B decreases drastically as the shell thickness increases, whereas it is independent in CdSe/ZnS NCs. The decreasing of the magnitude of the band A in the CdTe/CdSe NCs can be interpreted as the spatial overlap between the electron and hole wavefunctions decreases as the shell thickness increases, i.e. it is due to the type II configuration of the carriers (regime B in Fig. 1(b)). On the other hand, the magnitude of the band B in the CdTe/CdSe NCs is almost unchanged, which can be understood by considering that the energy level of the 1p-electron is much higher than that

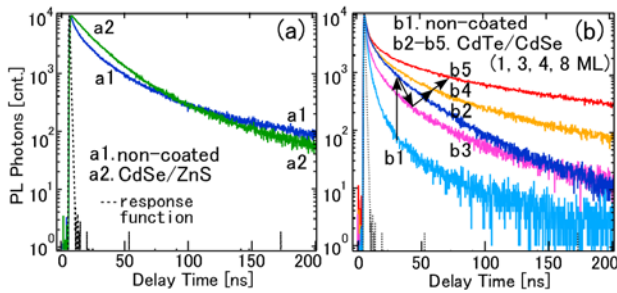


**Figure 3** (a) Curves a1 and a2 show PL decay profiles of non-coated CdSe NCs and CdSe/ZnS NCs dispersed in toluene solution, respectively. The broken line shows the response-function of the system. (b) Curves b1- b5. show PL decay profiles of non-coated CdTe NCs and CdTe/CdSe NCs.

of the  $1s$ -electron and thus the configuration of the  $1p$ - $1p$  electron-hole wavefunctions show little alterations.

From these results, we conclude that the CdTe/CdSe NCs with a thick shell are type II NCs, and that the origin of the bands A and B is the same as that of the CdSe/ZnS NCs. The PL band is assigned to a recombination of an electron-hole pair composed of a  $1s$ -electron and  $1s$ -hole.

For further insight into the properties of CdTe/CdSe NCs, we also have investigated the PL decay dynamics as a function of shell thickness.

Again we describe at first the PL decay profiles of type I CdSe/ZnS NCs for reference. Curves a1 and a2 in Fig. 3(a) show PL decay curves of non-coated CdSe and CdSe/ZnS NCs with 2.4 ML ZnS shell, respectively. The curve a1 is clearly not a simple single-exponential profile, i.e. the PL lifetime in non-coated CdSe NCs has a wide distribution. This distribution can be associated with surface states [11]. On the other hand, the decay curve a2 of the CdSe/ZnS NCs can be roughly approximated by a single exponential function, and its lifetime is estimated as 37 ns. In type I NCs, carriers are both confirmed in the core region, which prevents from accessing to surface states. It is also noted that the decay time of the coated CdSe/ZnS NCs is almost independent on shell thickness.

Next, we discuss the PL dynamics of the CdTe/CdSe NCs. Curves b1 to b5 in Fig. 3(b) show PL decay curves of non-coated CdTe NCs and CdTe/CdSe NCs with 1, 3, 4 and 8 ML shell, respectively. Strong shell thickness dependence of decay lifetime is observed in the CdTe/CdSe NCs. The lifetime of the non-coated NCs is increased by overcoating even the 1 ML shell (b1  $\rightarrow$  b2). Then, it decreases as the shell thickness increases in the range from 1 ML to 3 ML (b2  $\rightarrow$  b3). After a bit complicated decrease around 3ML, the PL lifetime increases again drastically (b3  $\rightarrow$  b4  $\rightarrow$  b5).

The lifetime components of the non-coated CdTe and the CdTe/CdSe NCs with 8 ML shell are estimated by a multi-exponential fitting; the results are 8.8 ns and 160 ns (major decay component for each), respectively. As for the large increase of the lifetime, it is also interpreted by considering

that, in the type II NCs, spatial overlap of electron and hole wavefunctions decreases as the shell thickness increases.

On the other hand, it is not clear yet why the increasing trend of PL lifetime is reversed around 1 to 3 ML. It may suggest that an electron or a hole confined in the CdTe NCs with a thin CdSe shell ( $\square$  1ML) tends to be trapped at part(s) of somewhat imperfect shell structure, which can work as shallow trap(s).

In summary, we synthesized non-coated CdTe and CdTe/CdSe core-shell NCs which possess systematic shell thicknesses (1, 2, 3, 4, 6 and 8 ML). Absorption and PL spectra, and also PL decay curves, of the NCs were reported. Large redshift and drastic decrease of magnitude of the lowest absorption band are observed in the NCs with a thick shell. These results suggest that the NCs with a thick shell are type II NCs, i.e. electrons and holes are localized in shell and in core, separately.

Strong shell thickness dependence of PL decay curves is also observed in the NCs. Dominant PL decay lifetimes of non-coated CdTe and CdTe/CdSe NCs with 8 ML shell are estimated as 8.8 ns and 160 ns, respectively. The prolonged lifetime is basically described by considering the spatial separation of electron and hole wavefunctions. On the other hand, the lifetime does not show monotonic increase as the shell thickness increases initially. This result may suggest that at the thin shell ( $\square$  1 ML) stage shells are rather imperfect.

**Acknowledgements** This research is partly supported by Iketani science and technology foundation.

## References

- [1] S. Kim, B. Fisher, H. J. Eisler, and M. Bawendi, *J. Am. Chem. Soc.* **125**, 11466 (2003).
- [2] V. I. Klimiv, S. A. Ivanov, J. Nanda, M. Achermann, I. Bezel, J. A. McGuire, and A. Piryatinski, *Nature* **447**, 441 (2007).
- [3] K. Hashizume, M. Matsubayashi, M. Vacha, and T. Tani, *J. Lumin.*, **98**, 49 (2002).
- [4] C. B. Murray, D. J. Norris, and M. G. Bawendi, *J. Am. Chem. Soc.*, **115**, 8706 (1993).
- [5] X. Peng, E. Troy, A. Wilson, A. P. Alivisatos, *Angew. Chem. Int. Ed. Engl.*, **36**, 45 (1997).
- [6] M. A. Hines and P. G. Sionnest, *J. Phys. Chem.*, **100**, 468 (1996).
- [7] D. V. Talapin, A. L. Rogach, A. Kornowski, M. Haase, and H. Weller, *Nano Lett.*, **1**, 207 (2001).
- [8] D. Schooss, A. Mews, A. Eychemüller, and H. Weller, *Phys. Rev.* **B49**, 17072 (1994).
- [9] T. Richard, P. Lefebvre, H. Mathieu, and J. Allègre, *Phys. Rev.* **B53**, 7287 (1996).
- [10] M. Kuno, J. K. Lee, B. O. Dabbousi, F. V. Mikulec, and M. G. Bawendi, *J. Chem. Phys.* **106**, 9869 (1997).
- [11] G. Schlegel, J. Bohnenberger, I. Potapova, and A. Mews, *Phys. Rev.* **B88**, 137401 (2002).